

# Particle size effect on the strength of rice husk ash blended gap-graded Portland cement concrete

D.D. Bui <sup>a</sup>, J. Hu <sup>b,\*</sup>, P. Stroeven <sup>b</sup>

<sup>a</sup> Hanoi University of Civil Engineering, 5 Giai phong Road, Hanoi, Viet Nam

<sup>b</sup> Faculty of Civil Engineering and Geosciences, Delft University of Technology, Stevinweg 1, 2628 CN Delft, The Netherlands

Received 24 March 2003; accepted 20 May 2004

## Abstract

Rice husk ash (RHA) has been used as a highly reactive pozzolanic material to improve the microstructure of the interfacial transition zone (ITZ) between the cement paste and the aggregate in high-performance concrete. Mechanical experiments of RHA blended Portland cement concretes revealed that in addition to the pozzolanic reactivity of RHA (chemical aspect), the particle grading (physical aspect) of cement and RHA mixtures also exerted significant influences on the blending efficiency. The relative strength increase (relative to the concrete made with plain cement, expressed in %) is higher for coarser cement. The gap-grading phenomenon is expected to be the underlying mechanism. This issue is also approached by computer simulation. A stereological spacing parameter (i.e., mean free spacing between mixture particles) is associated with the global strength of the blended model cement concretes. This paper presents results of a combined mechanical and computer simulation study on the effects of particle size ranges involved in RHA-blended Portland cement on compressive strength of gap-graded concrete in the high strength/high performance range. The simulation results demonstrate that the favourable results for coarser cement (i.e., the gap-graded binder) reflect improved particle packing structure accompanied by a decrease in porosity and particularly in particle spacing.

© 2004 Elsevier Ltd. All rights reserved.

**Keywords:** Computer simulation; Concrete compressive strength; Interfacial transition zone; Particle size ranges; Rice husk ash

## 1. Introduction

In high-performance concrete, the microstructure of the interfacial transition zone (ITZ) between the cement paste and the aggregate is of paramount importance for strength and durability of the material. The microstructure of the cement paste in the ITZ can be significantly improved by adding (super) fine materials, such as fly ash, silica fume, metakaolin, and rice husk ash (RHA). Rice husk ash is a highly reactive pozzolanic material produced by controlled burning of rice husk. The utilization of rice husk ash as a pozzolanic material in ce-

ment and concrete provides several advantages, such as improved strength and durability properties, reduced materials costs due to cement savings, and environmental benefits related to the disposal of waste materials and to reduced carbon dioxide emissions. Reactivity of RHA is attributed to its high content of amorphous silica, and to its very large surface area governed by the porous structure of the particles [1–4]. Generally, reactivity is favoured also by increasing fineness of the pozzolanic material [5–7]. However, Mehta [8] has argued that grinding of RHA to a high degree of fineness should be avoided, since it derives its pozzolanic activity mainly from the internal surface area of the particles.

Cements with higher fineness are applied in high-performance concrete (HPC). Traditionally, HPC is produced of low water to cement ratio mixtures (below

\* Corresponding author. Tel.: +31 15 278 2307; fax: +31 15 278 8162.

E-mail address: [j.hu@citg.tudelft.nl](mailto:j.hu@citg.tudelft.nl) (J. Hu).

0.4), to which a superplasticizer and a fine-grained pozzolanic material are added. The limited available space in the fresh state of such low water to cement ratio mixtures will be occupied after hardening by hydration products, which will also contain unhydrated cement regardless of the fineness of the cement [9]. Based on computer simulation, Bentz and Haecker concluded that in this situation coarser cements could yield equivalent long-term performance as compared to finer cements [10]. By blending finely ground RHA with such a coarser cement, higher packing densities near the aggregate grain interface can be expected, as a consequence, leading to improved behaviour of the blended systems [11,12]. This is a strategy emphasized in this paper.

It is well documented that the strengthening capability of a mineral admixture not only depends on the pozzolanic reactivity, but also on the filler effect. The latter feature is associated with the relative fineness of the filler material. In high-performance PC composites incorporating superfine particles, such as silica fume and carbon black, the filler effect has been demonstrated being even more pronounced than the pozzolanic effect [13,16]. Stroeve and Stroeve have demonstrated by means of computer simulation using the SPACE system [17–19] that the finest particles tend to concentrate near the aggregate–matrix interface, leading to reduced porosity and enhanced internal bonding capacity. Associated with the lower porosity was a *reduction in the thickness* of the ITZ. The strengthening effect extended, instead, over an ITZ of *increased thickness* [19]. The packing efficiency of a mineral admixture can be expected to depend, therefore, on the average *fineness gap* between the particles of the mineral admixture and of the cement. This will be investigated in this paper by employing the SPACE system for a computer simulation approach to this problem.

As a relatively soft and porous material, it is more cost effective to grind the RHA to larger fineness than to do so with the Portland cement in gap-graded binder

designs. Moreover, at a certain stage of grinding the RHA, the porous structure of the particles will collapse, thereby reducing the surface area of the RHA [11,20]. An increased fineness of the RHA, therefore, will ultimately result in a decline in water demand, and an enhanced filling capacity. This was not pursued, however, in the experiments of which the results are reported in this paper.

## 2. Materials and methods in mechanical approach

### 2.1. Materials and mixtures

#### 2.1.1. Cement

Two kinds of an ordinary Portland cement were employed, i.e., PC30 and PC40, which conform to Vietnamese standard TCVN 2682:1999. The cements originated from one clinker source but were pulverized to different degree of fineness. The physical properties of the cements are listed in Table 1.

#### 2.1.2. Rice husk ash

A Vietnamese type of rice husks was incinerated in a drum incinerator for production of the rice husk ash [21]. After combustion, the ash was finely pulverized by using a vibrating ball mill. Chemical composition and physical properties of the RHA are given in Table 2.

#### 2.1.3. Aggregates

Crushed basalt was used as coarse aggregate (9.5–19 mm). Sand with particles smaller than 0.6 mm and a fineness modulus of 1.1 was employed as fine aggregate. The grading and physical properties of the fine and coarse aggregates are shown in Table 3.

#### 2.1.4. Superplasticizer

A naphthalene-based superplasticizer, Mighty 100 of Kao Ltd., Japan, produced in powder form was used.

Table 1  
Properties of the cements

No	Properties	Test results		Standard TCVN 2682:1999	
		PC30	PC40	PC30	PC40
1	Normal consistency (%)	26	29	–	–
2	Setting time (minute)				
	(a) initial	95	85	≥ 45	≥ 45
	(b) final	190	175	≤ 375	≤ 375
3	Volumetric density (g/cm <sup>3</sup> )	3.14	3.15	–	–
4	Residue on 75 µm sieve (%)	10	4	<15	<12
5	Blaine specific surface area (cm <sup>2</sup> /g)	2700	3750	–	–
6	Compressive strength (MPa) <sup>a</sup>				
	(a) 3 days	16.2	22.6	>16	>21
	(b) 7 days	27.1	35.6	–	–
	(c) 28 days	38.5	47.7	>30	>40

<sup>a</sup> 40 × 40 × 160 mm prisms; cement:sand = 1:3; W/C = 0.5.

Table 2  
Chemical composition and physical properties of rice husk ash

Property	Rice husk ash
<i>Constituents (wt.%)</i>	
SiO <sub>2</sub>	86.98
Al <sub>2</sub> O <sub>3</sub>	0.84
Fe <sub>2</sub> O <sub>3</sub>	0.73
Na <sub>2</sub> O	0.11
K <sub>2</sub> O	2.46
CaO	1.40
MgO	0.57
Loss on ignition	5.14
<i>Physical properties</i>	
Volumetric density (g/cm <sup>3</sup> )	2.10
Mean particle size (μm)	5

Table 3  
Grading and physical properties of aggregates

	Cumulative percentage retained (%)	
	Crushed basalt (9.5/19)	Fine silica sand (0/0.6)
Sieve size (mm)		
19	5	–
9.5	98	–
4.75	100	–
2.36	100	–
1.18	100	–
0.6	100	–
0.3	100	15.9
0.15	100	92.4
Fineness modulus	7.03	1.08
Volumetric density (g/cm <sup>3</sup> )	2.92	2.61
Absorption (%)	0.6	1.2

### 2.1.5. Mixture proportioning

The aggregate for the mixtures consisted of a mixture of crushed basalt and of fine sand, with a sand content of 30% by weight. The result is a gap-graded mixture, due to the deficient particles in the 0.6 and 9.5 mm range.

Twenty four concrete mixtures were made, 12 mixtures for each of the two kinds of PC. Three levels of the water to binder ratio were investigated, i.e., 0.30, 0.32 and 0.34. The mixtures with water to binder ratio of 0.30 were made with a binder content of 550 kg/m<sup>3</sup> concrete. The binder content of all other mixtures was 500 kg/m<sup>3</sup>. Rice husk ash was used to replace 10%, 15% and 20% by mass of PC. The superplasticizer was added to all mixtures for obtaining high workability. In the mixtures with water to binder ratio of 0.34, the amount of superplasticizer was kept constant to investigate the influence of RHA on workability. Mixture proportions of the gap-graded concretes are given in Table 4.

### 2.2. Preparation of test specimens

Coarse and fine aggregates, and powder materials (cement, rice husk ash) were placed in correct proportions in a revolving concrete drum mixer. They were mixed in dry conditions for a period of two minutes, and for another three minutes after adding the water. The concrete mixture was mixed for a final three minutes after adding the superplasticizer to achieve the desired consistency. Slump and unit weight of the fresh concrete were determined immediately following the mixing procedure.

Cubes of 100 mm size were cast and compacted in two layers on a vibrating table. Each layer was vibrated for 10 s. The moulds were covered after casting with polyethylene sheets and moistened burlap for 24 h. Thereupon, the specimens were demoulded and cured in water at a temperature of 20 °C until the day of testing. Compressive strength of the concretes was determined at 1, 3, 7, 28 and 90 days, using three specimens per test age.

## 3. Experimental: results and discussion

### 3.1. Workability

All investigated mixtures had high slump values and were stable. Representative test results on workability are presented in Fig. 1. It is interesting to note that these highly workable gap-graded mixtures did not show segregation despite relatively low sand contents. Most probably, the relatively large volume content of very fine sand particles with diameters below 300 μm has contributed to a greater cohesiveness of the gap-graded concrete mixtures. The use of high binder contents at low water to binder ratios, and the addition of rice husk ash and superplasticizer, also promoted the cohesiveness of the gap-graded concrete mixtures. Fig. 2 reflects the superplasticizer demand for a constant workability of gap-graded mixtures made with the two kinds of Portland cement at water to binder ratio of 0.32. The finer cement (PC40) requires a higher superplasticizer dosage for achieving equal slump.

Fig. 1 reveals the influence of the RHA content, and the cement fineness on workability of gap-graded mixtures made with a water to binder ratio of 0.34. For the plain PC30 concrete, a superplasticizer dosage of 1% by mass of the cement is required to attain a slump of 210 mm. In case of the finer cement (PC40), the superplasticizer dosage is increased to 1.28% for obtaining approximately the same slump. A reduction in slump of the blended concrete mixtures is found when a part of the PC is replaced by RHA at equal superplasticizer content. This decline in slump increases with replacement level of cement by RHA.

Table 4

Mixture proportions of gap-graded concrete blended with RHA ( $\text{kg/m}^3$ )

W/B	Cement PC30	Cement PC40	RHA <sup>a</sup>	Water	SP <sup>b</sup>	Fine sand (0/0.6)	Crushed basalt (9.5/19)
0.3	550	—	—	165	5.60	550	1283
	495	—	55	165	5.80	546	1273
	468	—	82	165	6.10	543	1267
	440	—	110	165	6.30	540	1261
0.32	500	—	—	160	5.50	567	1324
	450	—	50	160	5.72	562	1313
	425	—	75	160	6.00	560	1307
	400	—	100	160	6.22	558	1301
0.34	500	—	—	170	5.00	560	1305
	450	—	50	170	5.00	555	1294
	425	—	75	170	5.00	553	1290
	400	—	100	170	5.00	551	1285
0.3	—	550	—	165	6.60	550	1283
	—	495	55	165	6.80	546	1273
	—	468	82	165	7.19	543	1267
	—	440	110	165	7.43	540	1261
0.32	—	500	—	160	6.50	567	1324
	—	450	50	160	6.76	562	1313
	—	425	75	160	7.08	560	1307
	—	400	100	160	7.36	558	1301
0.34	—	500	—	170	6.40	560	1305
	—	450	50	170	6.40	555	1294
	—	425	75	170	6.40	553	1290
	—	400	100	170	6.40	551	1285

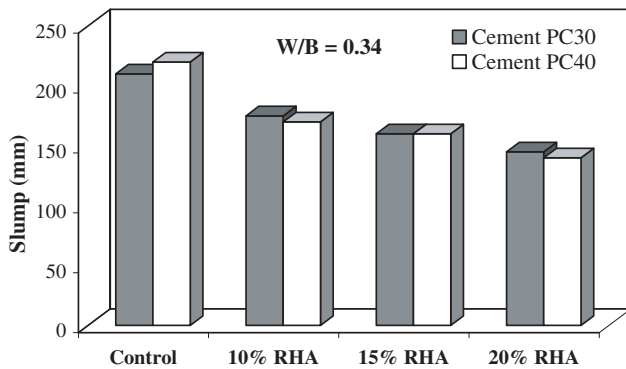
<sup>a</sup> RHA—rice husk ash.<sup>b</sup> SP—superplasticizer.

Fig. 1. Superplasticizer requirement for a constant workability of RHA blended gap-graded concretes made with cements of different fineness.

### 3.2. Compressive strength

#### 3.2.1. Concrete made with cement PC30

Compressive strength data of RHA blended concrete are shown in Table 5 to be higher than those of the plain cement concrete, irrespective of water to binder ratio and age. Compressive strength increases with blending percentage at corresponding values of water to binder ratio and age. This trend is pronounced for replacement levels up to 20%. Higher contents of RHA can be used without a strength loss. This will, however, cause an increase in the superplasticizer dosage required for attain-

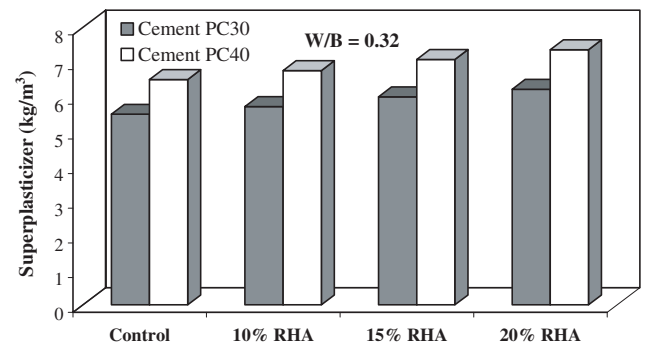


Fig. 2. Slump variation of gap-graded concretes made with cements of different fineness at constant superplasticizer content.

ing workable mixtures. Fig. 3 presents relative compressive strength data, defined as the ratio of the compressive strength of the RHA-blended concrete to the strength of the plain cement concrete with the same binder content and cured to the same age. The RHA blending increases the *relative strength* at all ages, however, most pronounced is the increase in the first 7 days. It is well known that coarse cements hydrate at lower rate and, therefore, produce lower early-age strengths as compared to finer cements made from the same clinker. This decline in early age strength gain is, in the authors' opinion, the result of higher porosity due to less efficient packing of more coarsely ground cement. Additionally, the reduction in volume of hydration products

Table 5  
Cube compressive strength of gap-graded concrete blended with RHA

Cement type	Binder composition cement–RHA (%) <sup>a</sup>	W/B <sup>b</sup>	Compressive strength (MPa)				
			1 day	3 days	7 days	28 days	90 days
Cement PC 30	100–00	0.3	22.0	43.5	53.6	63.5	71.7
	90–10	0.3	22.7	47.9	60.6	72.8	83.2
	85–15	0.3	22.9	49.0	62.5	75.1	84.9
	80–20	0.3	23.1	51.5	64.3	78.2	86.8
	100–00	0.32	20.9	41.3	51.0	59.6	66.8
	90–10	0.32	21.7	45.8	58.0	68.8	78.2
	85–15	0.32	21.8	46.5	61.2	72.2	81.5
	80–20	0.32	22.0	48.7	61.8	72.7	82.2
	100–00	0.34	18.9	39.9	49.8	57.9	64.9
	90–10	0.34	19.5	44.3	56.8	66.6	75.6
	85–15	0.34	19.7	45.2	57.6	67.2	75.8
	80–20	0.34	20.1	46.9	59.1	69.3	77.2
Cement PC 40	100–00	0.3	39.7	67.2	78.9	88.5	97.1
	90–10	0.3	34.7	60.8	83.6	95.2	104.1
	85–15	0.3	35.3	63.2	85.4	96.0	104.4
	80–20	0.3	37.5	66.5	86.0	98.1	106.5
	100–00	0.32	37.8	63.9	76.4	85.7	94.0
	90–10	0.32	32.1	58.9	80.6	91.6	100.3
	85–15	0.32	33.8	59.2	81.9	93.4	101.8
	80–20	0.32	34.2	60.7	82.8	94.3	103.3
	100–00	0.34	35.5	61.7	73.8	82.8	90.5
	90–10	0.34	29.9	57.6	78.9	89.7	98.5
	85–15	0.34	32.6	57.3	79.2	90.3	99.1
	80–20	0.34	31.1	59.2	80.3	91.1	100.1

<sup>a</sup> RHA—rice husk ash.

<sup>b</sup> W/B—water to binder ratio.

due to less favourable hydration rate is expected to result in a decrease in the early-age strengths. In RHA blended concrete, the  $\text{Ca}(\text{OH})_2$  formed during hydration of Portland cement at early ages is rapidly consumed due to the high pozzolanic reactivity of RHA. As a consequence, the hydration of cement is accelerated, and larger volumes of reaction products are formed. Moreover, the small RHA particles improve the particle packing density of the blended cement, leading to a reduced volume of larger pores and a more homogenous microstructure of the cement paste, particularly in the interfacial zone.

### 3.2.2. Concrete made with cement PC40

As expected—and confirmed by data in Table 5—concretes made with the fine cement (PC40) revealed considerable higher strengths than those made with the coarser cement (PC30). For instance, plain PC30 concrete with a cement content of  $550 \text{ kg/m}^3$  and a water to cement ratio of 0.30 yielded a 28-days compressive strength of 63.5 MPa. This strength level was raised to 88.5 MPa, when PC40 was applied under otherwise similar conditions. Partial cement replacement by RHA also significantly improved strength, although the effect was pronounced only at later ages. Fig. 4 and Table 5 reveal the compressive strength values of RHA blended concrete to be lower than those of plain cement concretes at ages up to 3 days. However, at later age, say

from 7 days onward, the blended concretes have higher compressive strength than those of the control concretes. Blending of RHA with the fine cement PC40 provides less efficient particle packing due to the narrower particle size range as compared to blending with the coarser PC30 cement. Hence, only a moderate contribution is given by the filler effect to early-age strength. To achieve optimum strength effects, the fineness of the RHA (or in general, the mineral admixture) should be attuned to that of the PC, i.e., average grain sizes of PC and admixture should be quite distinct, yielding gap-graded blends [22].

Table 5 and Figs. 3 and 4 clearly reveal the blending effects on the two different types of Portland cement concrete. PC40 is the finer cement, so that the plain concrete mixtures using this cement score better as to compressive strength in all cases. The hydration rate at early age of PC40 is also higher and thus is expected to achieve the superior 1 and 3 day's compressive strength values. The reaction rate of the RHA pozzolan is much lower, however. Therefore, blending by equal amounts of RHA puts the PC40 concrete at early ages in the more unfavourable position due to the diluting effect. This may not be compensated for by physical strength contributions, due to the significantly overlapping particle size distribution curves of the PC40 and the RHA. From this aspect, PC30 appears to be in a more advantageous position. In a quantitative sense, roughly similar strength

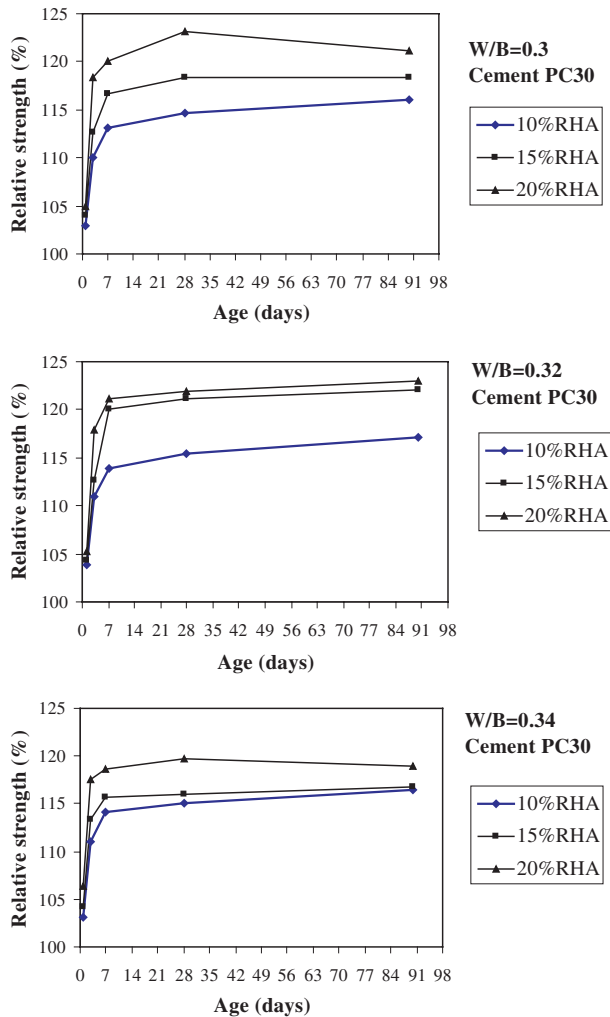


Fig. 3. Relative strength of gap-graded concrete made with RHA-blended cement PC30.

contributions at later ages come from the pozzolanic reaction. The physical contributions are different however, as a result of the better packing characteristics of the PC30 and the RHA. This is evidenced by the significant dependence of strength efficiency on blending percentage.

#### 4. Computer simulation approach

##### 4.1. Model materials and methods

Since the ITZ is the key issue in improving strength by blending, this zone constitutes the focal point in the computer simulation approach. A simulation system for particulate materials, with the acronym SPACE, is employed in this study. It is not based on a sequential procedure (from large to small particles) of randomly generated successive particle positions whereby overlap results in rejection of a particle; instead, the SPACE sys-

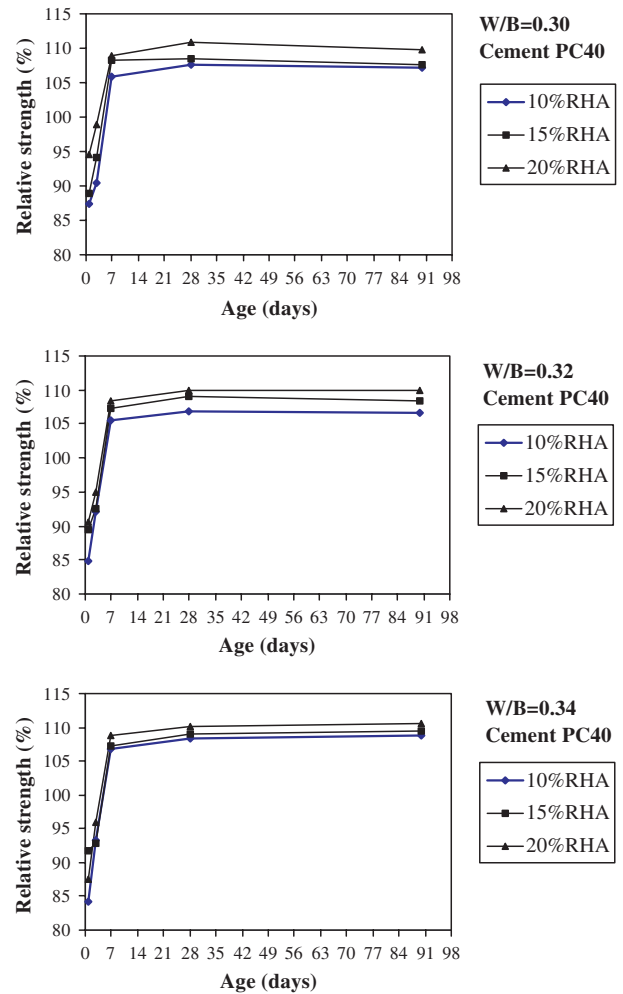


Fig. 4. Compressive strength of RHA blended gap-graded concrete made with Portland cement PC40.

tem encompasses a dynamic stage of the particle mixture in a (far) more dilute state. The requested density (corresponding to water–cement ratio) of the binder mixture can be obtained in a ‘natural’ way by gradually reducing the volume and using particle collision mechanics. This is a relatively realistic simulation of the production conditions in concrete technology. For a detailed description of the SPACE system and the algorithms for structure simulation, see [19,23]. Because of the dynamic set up of the system, it can deal with dilute to densely packed systems.

The medium value of the water to binder ratio of the experimental program, i.e.,  $W/B = 0.30$ , is adopted for the simulation. This implies volume fraction of *spherical* binder particles to occupy about 50% of the total volume. The size of the particles of the PC is made to closely match the so-called Rosin–Rammler particle size distribution function [9],  $G(d) = 1 - \exp(-bd^n)$ , where  $d$  is particle diameter,  $G(d)$  is the mass fraction of cement particles with diameter less than or equal to  $d$ . The constants  $n$  and  $b$  are derived from the exper-



Table 6  
Physical parameters of model cements

Model cement code	Size range ( $\mu\text{m}$ )	Blaine fineness ( $\text{m}^2/\text{kg}$ )	Rosin–Rammler parameters
PC30	1.5–23.04	248	$n = 1.03, b = 0.022$
PC30-RHA10	0.18–23	363	
PC30-RHA20	0.18–23	483	
PC40	1.5–18.93	329	$n = 1.10, b = 0.045$
PC40-RHA10	0.18–19	431	
PC40-RHA20	0.18–19	594	

imental data of cement particle size distribution. This function is generally accepted to represent the particle size distribution of ordinary PCs [9]. The simulation of the RHA is based on the sieve curve found in the experiments [11].

Table 6 presents some of the model data that characterize the particle mixtures used in the simulation experiments. The constants  $n$  and  $b$  of the Rosin–Rammler curves for PC30 and PC40 are given in column 3. The selected size ranges are presented in column 2. The designed size range of the RHA is 0.18–11  $\mu\text{m}$ . The upper border turned out to be 8.5  $\mu\text{m}$  in the generated mixtures. Partial replacement of the two types of PC with the relatively fine-grained RHA causes Blaine numbers to increase significantly, as shown also in column 3. Of course, the increase is largest for the coarser grained PC, i.e., 95% and 81% for PC30 and PC40, respectively, at 20% PC replacement level. This refinement of the blended mixtures is also revealed by the cumulative fractional volume density curves presented in Fig. 5.

Application of SPACE provides a cubical block of the particulate model material (blended Portland cement paste). To get information on the gradient perpendicular to the rigid interface surface (= container side) the block should be serially sectioned. The resulting sectional images should be subjected to quantitative image analysis. Material properties depend on geometrical–statistical features of the material structure. Structure-insensitive properties like mass or Young’s modulus only depend on volume fractions of the composing parts of a composite material. Density (or porosity) is therefore denoted as a composition parameter. In Contrast, a structure-sensitive property like crack initiation will appeal to material configuration, involving the mutual arrangement in space of the particles (size, spacing) [24,25]. For an elaborate discussion on this issue, see [19].

This paper deals with density and spacing. Density is the traditional approach to studying the ITZ. It is a relevant approach for assessing porosity when interested in certain concrete durability aspects. The quantitative image analysis approach should therefore offer information on volume fraction,  $V_V$ . A relevant 2-D parameter is the area fraction of particles,  $A_A$ , which is an unbiased estimator of  $V_V$ . When strength is at

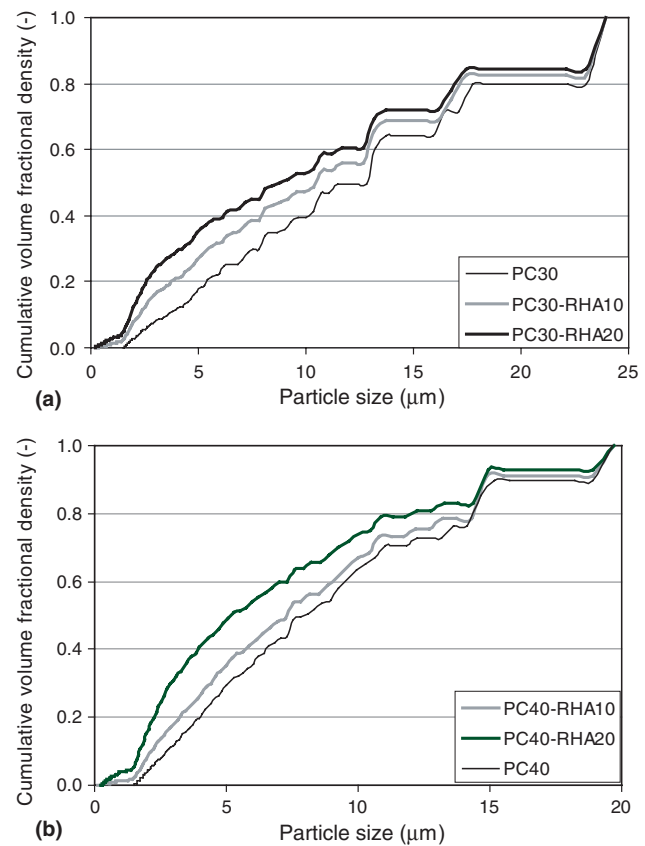


Fig. 5. Cumulative volume fractional density for investigated mixtures.

issue, a certain degree of structural sensitivity should be accepted. Only medium sensitivity will be encountered in the case of compression testing. The most relevant structural parameter is the mean free spacing,  $\lambda$ . It reveals only medium configuration sensitivity, and can easily be determined in a section from the expression:  $\lambda = 4(1 - V_V)/S_V$ . Herein,  $S_V$  is the specific surface area of the particles that is related to the perimeter length of the intersection circles per unit of area,  $L_A$ , by  $S_V = (4/\pi)L_A$ .

Following earlier studies [17,19], a global bonding capacity is used. When exceeded, the material is supposed to yield under compressive loadings. The global bonding capacity is—in analogy with van der Waals’ physical bond concept—taken proportional to the

reciprocal value to the third power of the mean free spacing (i.e.,  $\lambda^{-3}$ ).

#### 4.2. Results and discussion

A phenomenon detected earlier with SPACE, i.e., size segregation in the vicinity of a rigid interface [17,19], is shown in Fig. 6 for PC30 blended with 10% RHA. The successive size fractions—*only distinguished for illustration purposes*—have their peak contributions to total volume fraction at distances from the rigid interface that are proportional to the average sizes involved in the particle fractions. The total fractional volume density curve does not reflect this size segregation phenomenon. Instead, it shows a steep ascending branch at the left that is bending over to a plateau value at the right. The plateau value (= bulk density) extends over most of the cube width. Although the ITZ has no distinct boundaries, the plateau value can be imagined in accordance with [17,19] to start at about 1/3rd of maximum grain size, indicating the order of thickness of the ITZ for *compositional homogeneity*, i.e., for density or porosity. The grading inhomogeneity extends, however, outside this ITZ zone, as illustrated by the section patterns of Fig. 7, recorded at distances from the rigid interface of 1.3  $\mu\text{m}$ , 8.0  $\mu\text{m}$ , 23.3  $\mu\text{m}$  and 35.0  $\mu\text{m}$ , respectively. It can be expected, therefore, that the ITZ thickness for *grading homogeneity* will considerably exceed the one for density. Fig. 8 shows the fractional volume density curves for the investigated cases, demonstrating blending to reduce porosity in the layer immediately bordering the interface surface. Also, a tendency of reduced ITZ thickness by blending is observed. This confirms similar experiences when blending with silica fume. Bulk density is improved somewhat by blending, although only small differences were revealed between the two investigated partial PC replacement levels. No dramatic

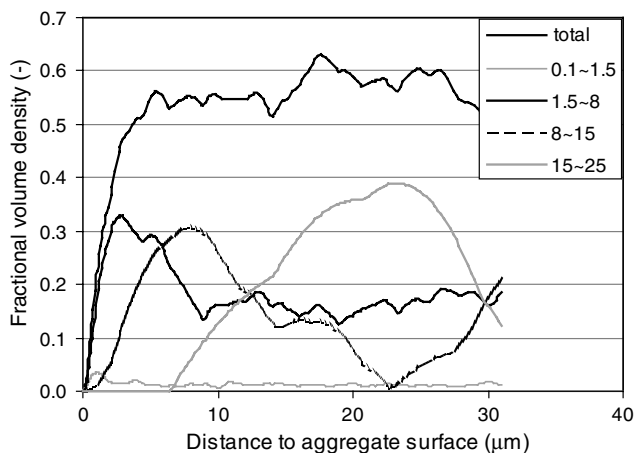


Fig. 6. Volumetric density of different size fractions (size range in  $\mu\text{m}$ ) of particles from model cement PC30 with 10% RHA replacement.

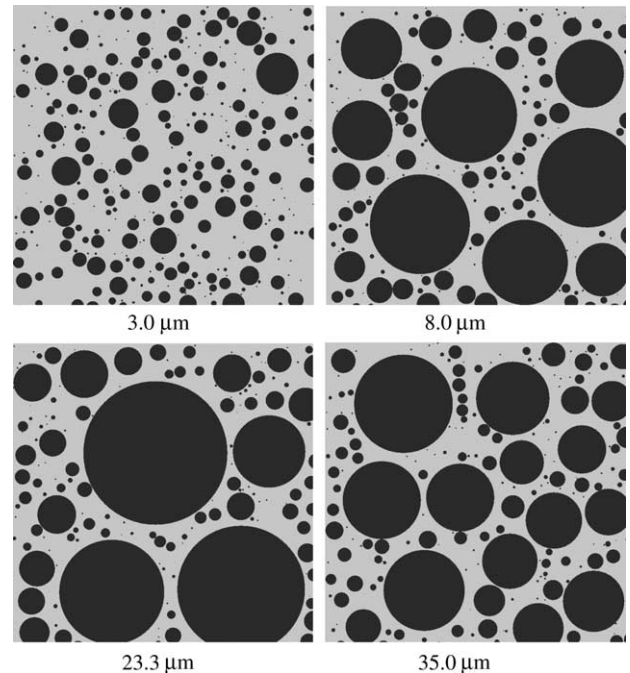
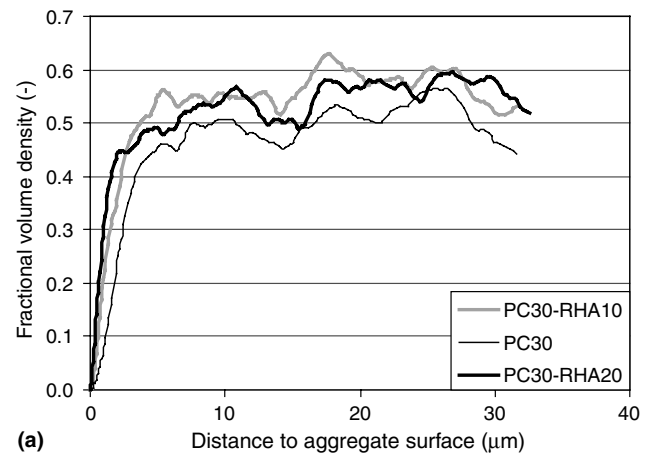
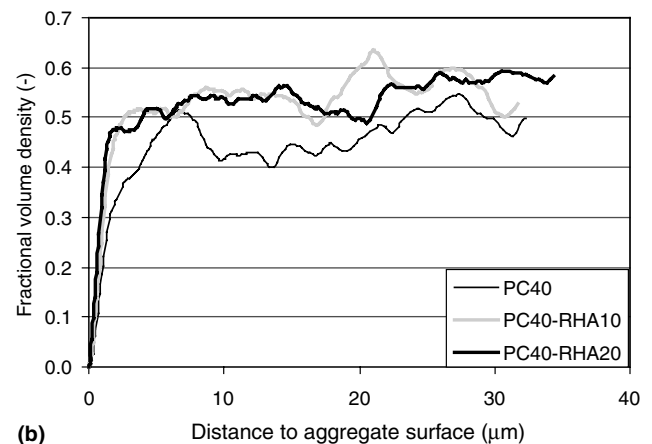


Fig. 7. Section images of model cement PC30 with 10% RHA replacement at specified distances from aggregate interface.



(a)



(b)

Fig. 8. Fractional volume density of model cements as function of distance to aggregate interface.



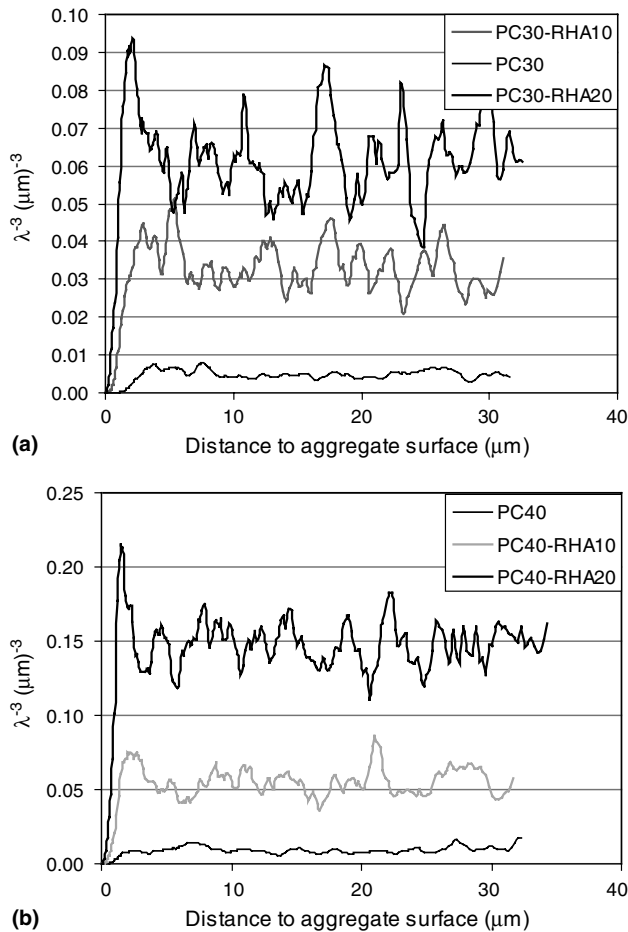


Fig. 9. Parameter proportional to global bond capacity of model cements as function of distance to aggregate interface.

effects of cement fineness on blending efficiency as to densification of the ITZ or bulk were found.

Fig. 9 presents the effects of blending on the global bonding capacity of the PC30 and PC40 model paste mixtures. The most remarkable feature is the disproportional increase in bond capacity in the layer bordering the rigid surface. In [19] this has also been found for HPC mixtures ( $W/B = 0.2$ ). In both cases, this effect should be attributed to the size segregation phenomenon. Further, in absolute terms, PC40 mixtures are superior as to strength capacity, but even in Fig. 9 it is obvious that the proportional improvements due to blending (= blending efficiency) are larger in the case of the coarser grained PC30. This is convincingly demonstrated in Fig. 10, displaying the bonding capacity of the blended mixtures normalized by the bulk bonding capacity of the respective types of Portland cement. Specifically at the 10% partial replacement level, the blending efficiency of PC30 is roughly 60% exceeding that of PC40. This is in qualitative agreement with the mechanical experiments. These differences considerably declined at the 20% partial replacement level. In all cases, blending efficiency is highest in the layer bordering the rigid

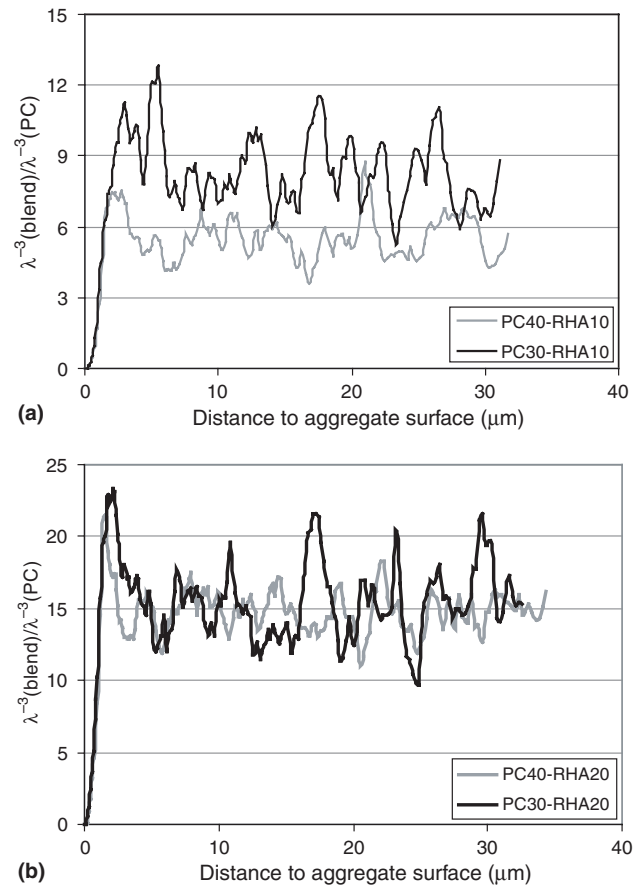


Fig. 10. Parameter proportional to global bond capacity of blended model cements normalized by respective plain cement bulk value as function of distance to aggregate interface.

interface. Since the global bonding capacity, as defined in this paper (supposed to be relevant for compressive strength testing), is depending on local grading and spacing characteristics, the associated ITZ will extend over a larger distance from the rigid interface than in the case of density homogeneity. This will get very pronounced particularly in the range of water to cement ratios between 0.2 and 0.3, as demonstrated in [14]. Because of its medium structure-sensitive character, bond estimates show larger scatter than density estimates, as can be concluded from a comparison of Figs. 8 and 9. To establish a proper estimate of the ITZ thickness in the latter case, a series of similar simulations should be performed (e.g., six in [19]). This is not the topic of this paper, however.

## 5. Conclusions

The results presented in this paper show that partial replacement of Portland cement by RHA leads to an increased water demand, which can be compensated for by the use of a superplasticizer. In addition, this

unfavourable effect is more pronounced for blends of RHA with finer cements (PC40). It has been argued before [11,12] that RHA can be ground to a fineness whereby the porous structure of the particles has collapsed. This would dramatically reduce water demand and the need to enhance the superplasticizer dosage.

Partial replacement of the PC with up to 20% RHA by mass yielded increased early-age compressive strength values only in the case of the gap-graded binder mixtures. RHA blending improved strength properties for both cement types. However, the gap-graded binder gave rise to significantly higher relative strength values for comparable cases. The magnitude of this blending efficiency as to compressive strength increases with the RHA content (in the studied partial replacement range). It is demonstrated by the computer simulation approach that the favourable results, particularly with the gap-graded binder, are reflecting improved particle packing leading to a decrease in porosity and particularly in spacing. This inevitably results in more significant *physical* contributions to strength, earlier demonstrated to be of significance in the lower range of *W/C* ratios [15,16]. Moreover, this probably caused the development of a more homogenous microstructure of the hydrated cement paste in the ITZ, yielding also a more favourable situation for the development of *chemical* contributions to strength.

## References

- [1] Mehta PK. Siliceous ashes and hydraulic cements prepared therefrom. US Patent 4105459, August 1978.
- [2] Mehta PK. Rice husk ash—a unique supplementary cementing material. In: Malhotra VM, editor. *Advances in concrete technology*. Ottawa: Centre for Mineral and Energy Technology; 1994. p. 419–44.
- [3] Cook DJ. Development of microstructure and other properties in rice husk ash—OPC systems. In: *Proceedings the 9th Australasian Conference on the Mechanics of Structures and Materials*. University of Sydney, Sydney, 1984. p. 355–60.
- [4] James J, Rao MS. Characterization of silica in rice husk ash. *Am Ceram Soc Bull* 1986;65(8):1177–80.
- [5] Kraiwood K, Chai J, Smith S, Seksun C. A study of ground coarse fly ashes with different finenesses from various sources as pozzolanic materials. *Cem Concr Compos* 2001;23:335–43.
- [6] Paya J, Monzo J, Peris-Mora E, Borrachero MV, Tercero R, Pinillos C. Early-strength development of Portland cement mortars containing air classified fly ashes. *Cem Concr Res* 1995;25(2):449–56.
- [7] Paya J, Monzo J, Borrachero MV, Peris E, Gonzalez-Lopez E. Mechanical treatment of fly ashes. Part III: studies on strength development on ground fly ashes—cement mortars. *Cem Concr Res* 1997;27(9):1365–77.
- [8] Mehta PK. The chemistry and technology of cement made from rice husk ash. In: *Proceedings UNIDO/ESCAP/RCTT Workshop on Rice Husk Ash Cements*, Peshawar, Pakistan, January 1979. Regional Centre for Technology Transfer, Bangalor (India), 1979. p. 113–22.
- [9] Taylor HFW. *Cement chemistry*. 2nd ed. London: Thomas Telford; 1997.
- [10] Bentz DP, Haecker CJ. An argument for using coarse cements in high-performance concretes. *Cem Concr Res* 1999;29:615–8.
- [11] Bui DD. Rice husk ash as a mineral admixture for high performance concrete. PhD thesis. Delft University Press, Delft, 2001.
- [12] Stroeven P, Stroeven M, Bui DD. Design principles of particle packing; application to supplementary cementing materials. In: Malhotra VM, editor. *Proceedings ACI 5th International Conference on Innovation in Design with Emphasis on Seismic, Wind and Environmental Loading, Quality Control and Innovation in Material/Hot-weather Concreting*. Farmington Hills: ACI; 2002. p. 43–60.
- [13] Mehta PK. Studies on the mechanisms by which condensed silica fume improves the properties of concrete. In: *Proceedings International Workshop on Condensed Silica Fume in Concrete*. Ottawa: CANMET; 1987. p. 1–17.
- [14] Goldman A, Bentur A. Bond effects in high-strength silica-fume concrete. *ACI Mater J* 1989;86(5):440–7.
- [15] Goldman A, Bentur A. The influence of microfillers on enhancement of concrete strength. *Cem Concr Res* 1993;23:962–72.
- [16] Detwiler RJ, Mehta PK. Chemical and physical effects of silica fume on mechanical behaviour of concrete. *ACI Mater J* 1989;86(6):609–14.
- [17] Stroeven P, Stroeven M. Computer simulation study of particle packing effects involved in design strategies for making HPC. In: Banthia N, Sakai K, Gjorv OE, editors. *Proceedings 3rd International Conference on Concrete under Severe Conditions*. The University of British Columbia, Vancouver, 2001. p. 1570–7.
- [18] Stroeven M, Stroeven P. Computer simulation of particle packing in cementitious systems. In: Malhotra VM, Helene P, Prudencio LR, Dal Molin DCC, editors. *High-Performance Concrete and Performance and Quality of Concrete Structures Proceedings 2nd CANMET/ACI International Conference*, Gramado, Brazil, ACI SP 186-19. Farmington Hills: ACI; 1999. p. 327–40.
- [19] Stroeven P, Stroeven M. Reconstructions by SPACE of the interfacial transition zone. *Cem Concr Compos* 2001;23:189–200.
- [20] Sugita S, Shoya M, Tokuda H. Evaluation of pozzolanic activity of rice husk ash. In: Malhotra VM, editor. *Proceedings 4th International Conference on Fly ash, Slag and Silica Fume in Concrete*, Istanbul, Turkey, May 1992. Detroit: ACI; 1993. p. 495–505.
- [21] Bui DD, Stroeven P. Workability and strength of lightweight aggregate concrete with rice husk ash. In: Stroeven P, Guo Z, editors. *Proceedings International Symposium on Modern Concrete Composites and Infrastructures*. Beijing, China, Delft: Delft University Press; 2000. p. 17–22.
- [22] Orange G, Dugat J, Acker P. DUCTAL: new high performance concretes. Damage resistance and micromechanical analysis. In: Rossi P, Chanvillard G, editors. *Fibre reinforced concretes BEFIB'2000*. Cachan: RILEM Publishing; 2000. p. 781–90.
- [23] Stroeven M. Discrete numerical model for the structure assessment of composite materials. PhD thesis. Delft University Press, Delft, 1999.
- [24] Freudenthal AM. *The inelastic behaviour of engineering materials and structures*. New York: Wiley; 1950.
- [25] Stroeven P. Some aspects of the micromechanics of concrete. PhD thesis. Delft University Press, Delft, 1973.